JOURNAL OF MAGNETIC RESONANCE **135,** 444–453 (1998)
ARTICLE NO. MN981555

Rovibrationally Averaged Nuclear Shielding Constants in OCS

Karol Jackowski,* Michał Jaszuński,† Włodzimierz Makulski,* and Juha Vaara‡

*Department of Chemistry, Warsaw University, Pasteura 1, 02 093 Warsaw, Poland; †Institute of Organic Chemistry, Polish Academy of Sciences, Kasprzaka 44, 01 224 Warsaw, Poland; and ‡Department of Physics and Measurement Technology, Linköping University, S-58 183 Linköping, Sweden, and NMR Research Group, Department of Physical Sciences, University of Oulu, FIN-90571 Oulu, Finland

Received February 11, 1998; revised June 15, 1998

The nuclear shielding constants in OCS are studied using ab initio theoretical methods and gas-phase NMR measurements. The shielding surfaces are calculated and the rovibrational effects and the resulting temperature dependence are analyzed. The temperature dependence of ^{13}C shielding in the gas phase is determined experimentally in the range 278–373 K. ^{13}C is the single nucleus for which the experimental data for the temperature dependence can be converted to a reference-independent scale, and good agreement of the measured and calculated ab initio results is observed. For ^{33}S, we discuss a new, more accurate absolute shielding scale. © 1998 Academic Press

Key Words: **shielding constants; OCS; rovibrational effects; temperature dependence.**

I. INTRODUCTION

The NMR spectrum of a molecule and the values of the parameters in the corresponding effective spin Hamiltonian depend on the temperature and on the interaction of this molecule with the environment. Ultimately, the comparison of accurate theoretical calculations with experimental results should take into account both these contributions. This is particularly important when accurate ab initio values are compared with precise measurements of the shielding constants as functions of density and temperature.

In this work we discuss rovibrational averaging and temperature dependence of oxygen, carbon, and sulfur nuclear shielding constants of the OCS molecule. For ^{13}C shielding, we compare our ab initio results with NMR data from our experiments performed in the gas phase. These new experimental values are derived by extrapolation to the limit of zero density and are therefore completely free from intermolecular effects. The ^{13}C magnetic shielding of the experimental reference—methane—as the absolute function of temperature has been studied in theory and experiment (*1, 2*) and referring to these results we may determine also the absolute temperature dependence of ^{13}C shielding for an isolated OCS molecule with the highest currently possible precision. Unfortunately, corresponding reference functions do not exist for the ^{17}O and ^{33}S NMR shielding.

Earlier experimental and theoretical results are used for comparison with our present data. References (*3, 4*) report the experimental NMR chemical shift for the ^{17}O nucleus in OCS in the gas and liquid phases, while Refs. (*5, 6*) contain the corresponding gas-phase data for ^{13}C. Solid-state data on the ^{13}C shielding tensor were presented in Ref. (*7*). On the contrary, ^{33}S continues to be a major challenge to NMR experimentalists, due to its large nuclear quadrupole coupling constant (NQCC). The ^{33}S shielding constant was estimated from an experimental spin–rotation constant and a model for diamagnetic shielding in Ref. (*8*). Reference (*9*), on the other hand, reported ab initio calculations of the diamagnetic shieldings and combined the results with experimental spin–rotation data to obtain both ^{13}C and ^{33}S shielding tensors. A few theoretical investigations of the OCS shielding tensors at the coupled Hartree–Fock level have been described (*7, 10–12*). More recently, the IGLO method has been used at the SCF and multiconfiguration SCF (MCSCF) level (*13*) and significant correlation corrections were observed. Reference (*4*) describes a correlated calculation of the ^{17}O shielding, performed at the coupled-cluster singles and doubles (CCSD) level.

We also report the ^{17}O and ^{33}S nuclear quadrupole coupling constants for OCS. Calculations of the electric field gradients at the nuclei were previously presented in Refs. (*11, 14*), and microwave spectroscopic experiments for the ^{17}O and ^{33}S NQCCs were described in Ref. (*15*).

II. GENERAL THEORY

A. Electronic Wavefunctions

For electron-rich molecules like OCS, with multiple bonds and lone pairs, at least the main correlation effects must be included in the calculation of the shielding constants, as the Hartree–Fock results are not sufficiently accurate (see, e.g., (*16*)). Various ab initio methods that describe correlation effects in such calculations have been developed. Since the perturbation considered is the external magnetic field, it was necessary to ensure simultaneously gauge invariance of the results. A formulation which permits the application of gauge including atomic orbitals (GIAOs) (*17*) for any correlated wavefunction has been described (*18*). The second-order

1090-7807/98 $25.00

Møller–Plesset perturbation scheme (MP2) (*19, 20*) is, similarly to the restricted Hartree–Fock (RHF) method, a convenient black-box approach. However, it is based on the single-determinant HF reference state and hence, just like the RHF itself, is not the optimal choice for studies of the geometry dependence of properties. Moreover, MP2 very often overestimates the correlation corrections for the shielding constants (*21*). Reliable results for shielding constants are obtained in the more advanced CCSD and CCSD(T) approaches (*22–24*). However, these methods are computationally expensive, in particular the more accurate CCSD(T) approach, and thus difficult to apply when the results are needed for numerous molecular geometries (for a study of diatomics, see Ref. (*25*)).

A compromise method, which describes well the potential energy surface in the neighborhood of the equilibrium and properties like the shielding constants, is to use an MCSCF function which takes into account the dominant correlation effects. In our calculations the shielding constants are determined applying MCSCF linear response theory; a detailed description of the response equations for the MCSCF approximation has been given in Ref. (*26*). An efficient scheme which combines the use of GIAOs and the MCSCF response approach in NMR shielding calculations has been developed; see, e.g., Ref. (*27*). We refer to these works for a presentation of the theory and its implementation in the Dalton program (*28*), which we have applied.

Various MCSCF wavefunctions were used in this work to study equilibrium geometries and shielding constants at the calculated equilibria. They are complete and restricted active space (CASSCF and RASSCF) wavefunctions differing in the choice of atomic basis set and MCSCF active space. For the property surfaces, we shall describe only the results obtained with two basis sets. Both of them are derived from the basis sets of Huzinaga (*29, 30*) (also called IGLO basis sets (*31*)) and have been successfully used in studies of NMR shielding constants (*27, 32*). The first basis of 114 CGTOs, called H III, is built from a [11*s*7*p*2*d*/7*s*6*p*2*d*] set for the carbon and oxygen atoms, and a [12*s*8*p*3*d*/8*s*7*p*3*d*] set for sulfur. The next, H IV, includes a [11*s*7*p*3*d*1*f*/8*s*7*p*3*d*1*f*] set of atomic orbitals for C and O and a [12*s*8*p*4*d*2*f*/9*s*8*p*4*d*2*f*] set for the S atom, with a total of 169 orbitals.

To describe the MCSCF wavefunctions, we use C_{2v} symmetry and specify the orbital subspaces for A_1, B_1, B_2, and A_2 symmetries, respectively. The SCF function has a (9, 3, 3, 0) occupation. In the three functions chosen to examine the property surfaces the core (5, 1, 1, 0) subspace is treated as inactive. The first two functions, called hereafter WF1 and WF2, include all the valence orbitals constructed primarily from atomic *s* and *p* shells in the active space. They are CASSCF functions with (6, 3, 3, 0) active orbitals, and approximately 60,000 determinants in the CI expansion. In this active space, the static correlation effects should be properly described; in particular the most important unoccupied antibonding π^* orbitals are treated on the same footing as the occupied orbitals. Different basis sets were used: H III for WF1 and H IV for WF2; thus we can estimate the convergence with the basis set comparing the relevant results. The third function, WF3, is a RASSCF wavefunction, including (5, 3, 3, 0) orbitals in the RAS2 subspace (with arbitrary occupation) and (2, 1, 1, 1) orbitals in the RAS3 subspace with a maximum of two electrons. These additional active orbitals affect mainly the description of the shielding of sulfur, having a large contribution of S atom 3*d* orbitals. Basis H IV was used in this calculation; hence WF2 and WF3 differ only in the description of correlation effects. The CI expansion for the WF3 function includes over 1,200,000 determinants for C_{2v} symmetry. For a nonlinear geometry, the number of determinants is approximately twice the number we have in the linear geometry wavefunction.

In addition to these three functions chosen to analyze the property surfaces, we have optimized the geometry for a number of other functions and considered the shielding at their equilibrium geometries. One wavefunction differed from WF2 in the basis set—we uncontracted all the *s*-type functions and added a set of tight *s* and *p* orbitals at the S atom. In another calculation, we used the H IV basis but allowed for electron excitations from three more "inner" (essentially core-type) orbitals. Both these changes have negligible effect on the equilibrium geometry and harmonic frequencies; also all the shielding constants at the respective equilibria differ by less than 1 ppm from the WF2 values. Larger changes of the results have been observed when we extended the active space to include more "outer" (diffuse) orbitals—but none of the other wavefunctions gave any systematic improvement of the properties we consider important for this study, that is, the geometries, force constants, and shielding constants. It appears that including more dynamic correlation is more important for other properties, e.g., the dipole moment.

Hence, we have finally selected only the three discussed functions for the property surface calculations. The first two functions differ only in the choice of the basis set, and the last includes more orbitals in the active space.

B. Rovibrational Averaging

The temperature dependence of an observable *a* can be described considering the rovibrational corrections to the equilibrium value, a_e. In the case of polyatomic molecules this can be done by averaging the Taylor series expansion of *a* in terms of the curvilinear internal displacement coordinates $\{R_i\}$, i.e., displacements of the bond lengths and angles from the equilibrium geometry, as described in Ref. (*16*). For OCS we have $\{R_i\} = \{\Delta r, \Delta r', \Delta\phi, \Delta\phi'\}$, and

$$\begin{aligned}\langle a\rangle^T \approx a_e &+ a_r\langle\Delta r\rangle^T + a_{r'}\langle\Delta r'\rangle^T \\ &+ \tfrac{1}{2}a_{rr}\langle(\Delta r)^2\rangle^T + \tfrac{1}{2}a_{r'r'}\langle(\Delta r')^2\rangle^T \\ &+ a_{rr'}\langle\Delta r\Delta r'\rangle^T + a_{\phi\phi}\langle(\Delta\phi)^2\rangle^T, \qquad [1]\end{aligned}$$

where Δr and $\Delta r'$ refer to displacements in the O═C and C═S bond lengths, respectively; $\Delta\phi$ is the bond angle; and angular brackets $\langle\ \rangle^T$ denote thermal average at the temperature T in question. There are two independent bending coordinates $\Delta\phi$ and $\Delta\phi'$ but $a_{\phi\phi} = a_{\phi'\phi'}$ and for their averages, $\langle(\Delta\phi)^2\rangle^T = \langle(\Delta\phi')^2\rangle^T$. The derivatives $a_i = (\partial a/\partial R_i)_e$ and $a_{ij} = (\partial^2 a/\partial R_i \partial R_j)_e$ are independent of temperature and atomic masses within the Born–Oppenheimer approximation. Numerical experience indicates that the third and higher order terms omitted from Eq. [1] can be neglected (*33*).

The average linear and quadratic internal coordinates can be calculated from the cubic anharmonic force field of the molecule, i.e., the harmonic (second order) and third order force constants appearing in the expression

$$\begin{aligned} V \approx & \tfrac{1}{2} f_{rr}(\Delta r)^2 + \tfrac{1}{2} f_{r'r'}\ (\Delta r')^2 + f_{rr'}\Delta r\Delta r' \\ & + \tfrac{1}{2} f_{\phi\phi}[(\Delta\phi)^2 + (\Delta\phi')^2] \\ & + \tfrac{1}{6} f_{rrr}(\Delta r)^3 + \tfrac{1}{6} f_{r'r'r'}\ (\Delta r')^3 \\ & + \tfrac{1}{2} f_{rrr'}(\Delta r)^2\Delta r' + \tfrac{1}{2} f_{rr'r'}\Delta r\ (\Delta r')^2 \\ & + \tfrac{1}{2} f_{r\phi\phi}[\Delta r(\Delta\phi)^2 + \Delta r(\Delta\phi')^2] \\ & + \tfrac{1}{2} f_{r'\phi\phi}[\Delta r'\ (\Delta\phi)^2 + \Delta r'\ (\Delta\phi')^2], \end{aligned} \qquad [2]$$

valid for a linear triatomic molecule. In terms of the rectilinear mass-dependent normal coordinates Q_k, the averages required in Eq. [1] can be approximated as

$$\begin{aligned} \langle R_i\rangle^T &\approx \sum_k L_i^k\langle Q_k\rangle^T + \frac{1}{2}\sum_k L_i^{kk}\langle Q_k^2\rangle^T \\ \langle R_iR_j\rangle^T &\approx \sum_k L_i^kL_j^k\langle Q_k^2\rangle^T, \end{aligned} \qquad [3]$$

where R_i is Δr, $\Delta r'$, $\Delta\phi$, or $\Delta\phi'$ and L_i^k and L_i^{kk} are so-called **L** tensor elements (*34*). $\langle Q_k\rangle^T$ and $\langle Q_k^2\rangle^T$ are obtained using the known approximation of Toyama *et al.* (*35*), as implemented in the AVIBR program (*36*). $\langle Q_k^2\rangle^T$ are computed from the zeroth order wavefunctions of the harmonic oscillators, i.e., over the harmonic vibrations of the molecule: $\langle Q_k^2\rangle^T = \langle Q_k^2\rangle^T_{\rm vib}$. For the calculation of $\langle Q_k\rangle^T$, the first order rovibrational wavefunctions perturbed by the cubic anharmonic terms of the vibrational potential energy and by the linear terms of the vibration–rotation interaction are used. Consequently, $\langle Q_k\rangle^T = \langle Q_k\rangle^T_{\rm vib} + \langle Q_k\rangle^T_{\rm rot}$ (and, e.g., $\langle\Delta r\rangle^T = \langle\Delta r\rangle^T_{\rm vib} + \langle\Delta r\rangle^T_{\rm rot}$), where the "rot" term comes from centrifugal distortion. Although the latter contribution to $\langle a\rangle^T$ is usually small at any given T, the effect on the temperature dependence of the observable may be significant (*16, 37*); therefore it cannot be neglected.

For each of the electronic wavefunctions applied in this work, the geometry has been optimized and the potential energy and molecular property surfaces (nuclear shielding and its anisotropy for each nucleus, and quadrupole coupling constants for O and S) were determined from a set calculations performed for 18 distinct geometries of the molecule. These correspond to the optimized equilibrium plus 10 linear and 7 bent geometries, defined in terms of the R_i (thus different Cartesian geometries are selected for each wavefunction). The property derivatives a_r, $a_{r'}$, etc., were least-squares fitted to a full third order Taylor series expression around the equilibrium geometry, whereas in the case of the potential energy, also the three all-diagonal fourth order force constants (f_{rrrr}, $f_{r'r'r'r'}$, and $f_{\phi\phi\phi\phi}$) were included in the fit. The points used in the fit were chosen to reside within ± 2 $(\langle R_i^2\rangle^{300\ \rm K})^{1/2}$ of the equilibrium geometry. The property averaging was performed using Eq. [1], i.e., the full second order expression, where the averages of the internal coordinates were calculated using the full third order expression of the intramolecular potential energy (Eq. [2]).

III. EXPERIMENTAL

The NMR signal for a molecule, even in the gas phase, is affected by intermolecular effects and by rovibrational motion. Both contributions are temperature dependent, so the nuclear shielding may be written as an expansion in powers of density (*38*),

$$\sigma(T,\ \rho) = \sigma_0(T) + \sigma_1(T)\rho + \sigma_2(T)\rho^2 + \cdots, \qquad [4]$$

where ρ is the density of the gas, $\sigma_0(T)$ is the temperature-dependent shielding in the limit of zero pressure, and $\sigma_1(T)$ is a measure of the effects on nuclear shielding due to binary collisions. The higher order terms, starting from $\sigma_2(T)$, are negligible for low-density samples. The effects of vibrational averaging and centrifugal distortion on the nuclear shielding in an isolated molecule are described by $\sigma_0(T)$, and this is what we compare with the ab initio results.

It is well known that the most precise measurements of NMR chemical shifts can be obtained when the magnetic field is stabilized by the lock system. It allows removing all the instrumental sources of resonance frequency changes but incorporates the temperature dependence of lock and reference signals into the final results (*39*). We shall assume here that the absolute temperature dependence of ^{13}C shielding in methane is known with sufficient accuracy from the work of Raynes *et al.* (*1*) and the CH_4 signal can serve as the temperature reference standard. Test CASSCF calculations using a large GIAO basis set confirm that for CH_4 the terms depending on the symmetric stretch are well described in the SCF approximation.

Natural abundance ^{13}C NMR spectra were obtained at 125.88 MHz in a Varian UNITYplus-500 FT NMR spectrom-

TABLE 1
Equilibrium Geometry and Harmonic Vibration Frequencies of OCS[a]

	WF1	WF2	WF3	CCSD(T)	Expt[b]	
$r = r_{CO}$	1.1575	1.1583	1.1579	1.1583	1.1554	1.1562
$r' = r_{CS}$	1.5844	1.5795	1.5694	1.5690	1.5620	1.5614
ω_1	842.50	850.02	871.89	871.7	875.7	875.3
ω_2	520.61	528.20	550.75	523.8	523.6	524.4
ω_3	2082.50	2088.62	2091.84	2094.5	2092.5	2093.7

[a] R in Å and ω (for the isotopomer $^{16}O{=}{}^{12}C{=}{}^{32}S$) in cm^{-1}. CCSD(T) data taken from (*41, 42*).
[b] Experimental data from Ref. (*47*) (left column) and Ref. (*48*) (right column).

eter in sealed 4-mm-o.d. glass tubes about 5 cm long and containing pure carbonyl sulfide (OCS) or methane (CH_4) at low densities (pressure 1–9 atm). All gas samples were prepared by the condensation of pure gases (Aldrich) from the calibrated part of a vacuum line. The volumes of sample tubes and the vacuum line were measured using mercury. The gas samples were fitted into the standard 5-mm-o.d. thin-walled NMR tubes (Wilmad 528-PP) with liquid toluene-d_8 in the annular space. The CD_3 group in toluene-d_8 was used for the lock system. The ^{13}C chemical shifts were measured relative to the fixed frequency of a TMS signal. The spectra of methane were recorded using the broadband-decoupled INEPT (insensitive nuclei enhancement by population transfer) experiments (*40*) which were optimized in order to minimize temperature effects in the samples. The temperature was stable within $\pm 0.5°$ during all the measurements, as verified with the standard samples of methanol and ethylene glycol. A single ^{13}C spectrum had a spectral window of 1400 Hz and a resolution of at least 0.2 Hz/point and required an accumulation time from 5 min to a few hours. Some peaks of the spectra were fitted to Lorentzians for more precise measurements of chemical shifts in the low-density samples. Usually six samples of various density were measured at each temperature in order to extrapolate accurately the results to zero density.

IV. RESULTS AND DISCUSSION

A. Energy

As a first step in the discussion of the results we present a comparison of our potential with other theoretical and experimental data. The values characterizing the optimized equilibrium—internuclear distances and harmonic frequencies—are shown in Table 1. Generally, the agreement with experiment increases from WF1 to WF2 to WF3, and all parameters, apart from the harmonic bending frequency, ω_2, are within 0.5% of the experiment at the final WF3 level (with WF1 and WF2 better values of ω_2 were obtained than with WF3). The accuracy of WF3 results other than ω_2 is comparable with CCSD(T)/cc-pVQZ numbers (*41, 42*). We have performed the calculation of the shielding surfaces for three functions, WF1, WF2, and WF3; thus we may estimate the relationship between the differences in the potential and the differences in the rovibrational effects on the shielding.

Table 2 displays the theoretical and experimental anharmonic force field parameters. Our results are in much better agreement with CCSD(T)/cc-pVQZ than with experimental data, particularly for the cubic (and included quartic) constants. This reflects, most likely, the technique of the fitting (number and type of constants included) and the larger experimental uncertainty in these parameters as compared to the harmonic force field (*42*). The difference between the values of ω_2 from WF3 and experiment is also noticeable in the results for the corresponding force constant, $f_{\phi\phi}$.

In addition, the quality of our basis set is confirmed by a comparison with two CCSD(T) calculations, of Refs. (*41, 42*). Our WF3 results shown in Table 2 agree better with the more recent larger basis set cc-pVQZ results than with the previous cc-pVTZ values for all but one ($f_{r'\phi\phi}$) parameter of the force field.

To summarize, both the basis set and the active space of the WF3 function appear to be sufficiently large for our purposes. The geometry and force field parameters agree well with experimental and most accurate ab initio values. The changes of the calculated parameters between the more approximate WF1 and WF2 and the WF3 wavefunction are not very large, and primarily related to $r' = r_{CS}$, in agreement with the character of the added active space orbitals.

We conclude this section recalling that our primary goal is an investigation of temperature dependence of the shielding constants. Thus, in principle we can combine a potential taken from any source with any calculated property surface. Since our own potentials are accurate enough, it is obviously more consistent to use for each computed property surface the potential obtained with the corresponding wavefunction, and this is how all our results for the shielding discussed below were obtained. We have verified in a test calculation that using instead of the WF1 potential another one, derived from the CCSD(T)/cc-pVTZ calculation (*41*), has a minimal effect on the rovibrationally averaged shieldings calculated with the WF1 shielding derivatives (the difference at 300 K is 0.1 ppm for O, 0.03 ppm for C, and 0.3 ppm for S).

TABLE 2
Anharmonic Force Field of OCS[a]

	WF1	WF2	WF3	CCSD(T)	Expt	Units
f_{rr}	16.27	16.29	16.25	16.12	16.01	aJ/Å^2
$f_{r'r'}$	6.82	6.94	7.34	7.41	7.51	aJ/Å^2
$f_{rr'}$	1.06	1.05	1.12	1.01	0.99	aJ/Å^2
$f_{\phi\phi}$	0.65	0.67	0.72	0.66	0.65	aJ/rad^2
f_{rrr}	−115.52	−114.23	−113.02	−113.19	−95.20	aJ/Å^3
$f_{r'r'r'}$	−40.17	−41.18	−43.24	−43.36	−46.50	aJ/Å^3
$f_{rrr'}$	−2.77	−2.81	−2.97	−2.67	−3.47	aJ/Å^3
$f_{rr'r'}$	−1.24	−1.13	−1.62	−1.17	0.64	aJ/Å^3
$f_{r\phi\phi}$	−0.87	−0.81	−0.83	−0.82	−3.09	aJ/(Å rad^2)
$f_{r'\phi\phi}$	−0.98	−1.08	−1.03	−0.96	−0.31	aJ/(Å rad^2)
f_{rrrr}	670.49	666.47	794.65	669.24	317.10	aJ/Å^4
$f_{r'r'r'r'}$	193.53	207.05	213.68	192.97	205.20	aJ/Å^4
$f_{\phi\phi\phi\phi}$	1.89	1.24	1.00	1.17	2.16	aJ/rad^4

[a] Experimental data taken from Ref. (*47*) and CCSD(T)/cc-pVQZ from (*42*).

B. Shielding—Absolute Values and Anisotropies

The shielding constants and anisotropies obtained using the present reference wavefunctions at their respective equilibrium geometries are listed in Table 3. All the results of a recent CCSD calculation (*4*) are also shown in Table 3. For comparison, we give also the SCF and MP2 shielding constants obtained with the same basis set and at the same geometry as the quoted CCSD values: SCF: σ(O) = 79.83, σ(C) = 13.23, σ(S) = 790.08 ppm; and MP2: σ(O) = 118.94, σ(C) = 47.36, σ(S) = 827.44 ppm. Thus, MP2 overestimates significantly all the correlation corrections with respect to the more accurate CCSD method, in agreement with the usual trends.

From the small (below 1 ppm) differences between our WF1 and WF2 results it may be concluded that even the smaller of the two basis sets is already converged. These two functions are similar to the functions used by van Wüllen and Kutzelnigg (*13, 43*) in their MCSCF-IGLO calculations. The results are also similar; for example, σ(O) = 105.91, σ(C) = 40.06, and σ(S) = 822.67 ppm for basis H IV in Ref. (*43*); the differences arise since we optimize the geometry and apply GIAOs. WF3

TABLE 3
Shielding Constants and Anisotropies at the Equilibrium Geometry and with Rovibrational Averaging[a]

		At equilibrium geometry			Rovibrationally averaged[b]	
	CCSD[c]	WF1	WF2	WF3	WF3	Expt
σ(O)	103.42	98.15	98.14	105.42	98.77	91 ± 3,[d] 86 ± 3,[e] 88.1[c]
σ(C)	34.06	38.30	37.72	35.06	33.26	30.0 ± 1.3,[f] 31.2,[g] 35.1 ± 3[h]
σ(S)	806.64	809.27	808.92	822.32	809.05	843 ± 12,[i] 817 ± 12[j]
$\Delta\sigma$(O)	467.76	474.75	474.40	463.94	473.72	
$\Delta\sigma$(C)	381.52	374.37	374.95	378.95	380.71	383.3,[g] 365 ± 3[h]
$\Delta\sigma$(S)	382.24	378.94	379.15	359.44	374.73	329 ± 18[g]

[a] Shieldings and anisotropies in ppm. The nuclear shielding anisotropy is defined as $\Delta\sigma = \sigma_{zz} - \frac{1}{2}(\sigma_{xx} + \sigma_{yy})$, with the molecule aligned along the z axis. For the equilibrium geometries, see Table 1.

[b] Rovibrational averaging performed at T = 303 K. The isotopomers ^{17}O═^{12}C═^{32}S, ^{16}O═^{13}C═^{32}S, and ^{16}O═^{12}C═^{33}S were considered for O, C, and S shielding tensors.

[c] Results from Ref. (*4*). The experimental shielding in solution; the chemical shift with respect to CO converted to absolute shielding of oxygen using $\sigma^{300\ K}$ (CO) = −59.3 ± 2 ppm (*44*).

[d] Gas-phase measurement (*3*). Converted to absolute scale as in footnote *c*. Similarly, 90.9 in Ref. (*4*).

[e] As footnote *d* but in solution (*3*).

[f] Gas-phase result from Ref. (*6*).

[g] Ref. (*9*). A combination of experimental spin–rotation constant and theoretical diamagnetic shielding.

[h] Low-temperature solid-state measurement (*7*) with respect to TMS reference (σ_C (TMS) = 188.1 ppm (*6*)).

[i] Ref. (*8*). A combination of experimental spin–rotation constant and estimated diamagnetic shielding.

[j] See text. A combination of experimental spin–rotation constant and calculated diamagnetic shielding.

TABLE 4
Derivatives of Nuclear Shielding in OCS with Respect to Internal Coordinates

	Oxygen			Carbon			Sulfur			
	WF1	WF2	WF3	WF1	WF2	WF3	WF1	WF2	WF3	Units
σ_r	−381.7	−383.7	−351.6	−173.8	−172.1	−187.8	−756.8	−752.0	−761.5	ppm/Å
$\sigma_{r'}$	−366.4	−365.8	−361.6	−92.3	−93.5	−82.9	−655.1	−635.9	−566.5	ppm/Å
σ_{rr}	−1510.4	−1506.4	−1412.2	−165.1	−171.5	−273.6	−618.0	−574.7	−528.0	ppm/Å^2
$\sigma_{r'r'}$	−139.6	−145.2	−135.4	−189.2	−180.8	−179.9	−4614.8	−4462.2	−4140.5	ppm/Å^2
$\sigma_{rr'}$	−800.2	−790.1	−780.4	−180.8	−180.2	−188.8	−237.5	−248.0	−101.5	ppm/Å^2
$\sigma_{\phi\phi}$	−246.8	−247.8	−261.8	−16.3	−17.2	−25.6	−572.7	−551.2	−321.8	ppm/rad^2

brings the C and O shielding constants (and anisotropies, see below) close to the CCSD results, while σ(S) moves slightly away from the CCSD value.

The gas-phase experiment by Wasylishen *et al.* (*3*) resulted in $\sigma(O) = 91 \pm 3$ ppm (using the oxygen shielding scale from a recent CCSD(T) calculation (*44*)), whereas our rovibrationally averaged value lies approximately 8 ppm above this value.

Apparently, we similarly slightly overestimate the carbon shielding constant; compare our rovibrationally averaged 33.26 ppm (WF3) with 30.0 or 31.2 ppm derived from gas-phase experimental data (*6*, *9*). The low-temperature solid-state measurement (*7*) gives a larger shielding constant than that observed in the gas phase; the medium effect is of opposite sign than usually.

The quoted experimental value for σ(S), 843 ± 12 ppm (*8*), is larger than our present result. However, this value was obtained with a crude estimate of the diamagnetic contribution. Using the same spin–rotation value as Wasylishen *et al.*, but our own diamagnetic contribution, we obtain 817 ± 12 ppm (WF3, the differences with other wavefunctions are below 0.5 ppm). This should be—as the diamagnetic contribution is, in contrast to Ref. (*8*), calculated, not estimated—a more accurate value of absolute ^{33}S shielding in OCS, which might be used to set the shielding scale. In addition, this result confirms the accuracy of our calculations; the total value of the shielding is in good agreement with the results in Table 3.

The nuclear shielding tensor of a linear molecule is completely determined by the shielding constant and its anisotropy, $\Delta\sigma = \sigma_{zz} - \frac{1}{2}(\sigma_{xx} + \sigma_{yy})$, where z is the symmetry axis. The equilibrium and rovibrationally corrected (at 303 K) values of the O, C, and S anisotropies are listed in Table 3. To our knowledge, there is no experimental result for the ^{17}O shielding anisotropy in OCS. The low-temperature Ar matrix isolation experiment (*7*) for ^{13}C resulted in $\Delta\sigma(C) = 365 \pm 3$ ppm, significantly below the gas-phase result of 383.3 ppm (*9*). Our calculations are in good agreement with the latter experiment. For S our result, 374.7 ppm, is larger than an early estimate based on spin–rotation and theoretical data (*9*).

C. Shielding—Temperature Dependence

The derivatives of the shielding constants with respect to the internal coordinates, used in the rovibrational averaging, are given in Table 4. Figures 1, 2, and 3 display the total rovibrational contribution to the shielding constant of O, C, and S, respectively. It may be seen from the figures that although the differences between the equilibrium values (assumed to define zero for the scale of the figures) and 170 K are significant, the change in the range 170–420 K is much smaller and fairly similar for all the approximations. This indicates that the contribution of the zero-point vibrational motion is large in comparison to the part arising from vibrational excitations at this temperature range. The magnitude of the shielding deriv-

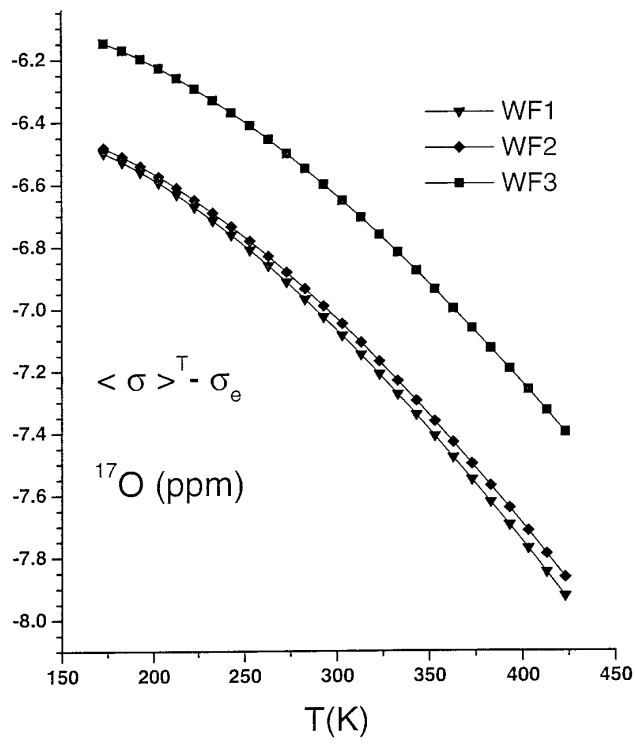

FIG. 1. Rovibrational contribution to the oxygen nuclear shielding constant in OCS as a function of temperature. Isotopomer $^{17}O{=}^{12}C{=}^{32}S$.

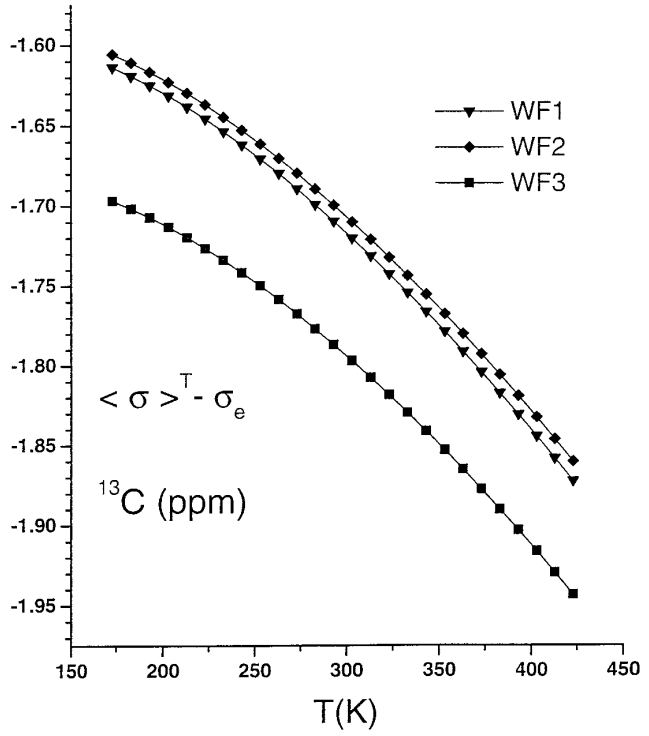

FIG. 2. Rovibrational contribution to the carbon nuclear shielding constant in OCS as a function of temperature. Isotopomer $^{16}O{=}^{13}C{=}^{32}S$.

atives and, consequently, that of the rovibrational contribution to shielding reflects the chemical shift range of the element in question. WF1 and WF2 give essentially identical results, while WF3 deviates slightly from them, particularly for S.

The contributions of the different terms in the full second order expansion of shieldings, Eq. [1], largely parallel those found for CSe_2 (*16*). Looking at the situation at 303 K, for instance, for oxygen the two first order terms (with σ_r and $\sigma_{r'}$) each contribute slightly below one-third of the total rovibrational shielding, while approximately one-third comes from bending, i.e., a second order term. Bending is also very important for the other terminal atom, S, but here also another second order term, $\frac{1}{2}\sigma_{r'r'}\langle(\Delta r')^2\rangle^{303\ \mathrm{K}}$, gives a large contribution of a quarter of the total $[\langle\sigma(\mathrm{S})\rangle^{303\ \mathrm{K}} - \sigma_e(\mathrm{S})]$. This is due to the large $\sigma_{r'r'}$ derivative for S (see Table 4). The first order terms yield only half of the total rovibrational correction. For the central carbon atom the bending mode is not very important, and the first order terms dominate: half of $[\langle\sigma(\mathrm{C})\rangle^{303\ \mathrm{K}} - \sigma_e(\mathrm{C})]$ arises due to the change of the C=O bond length, while approximately one-quarter comes from the other bond. This is due not only to the relatively large vibration amplitude of the bond involving the lighter terminal atom O, but also to the fact that the derivative σ_r (C) is more than twice as large as $\sigma_{r'}$ (C). The centrifugal terms $\sigma_r\langle\Delta r\rangle_{\mathrm{rot}}^{303\ \mathrm{K}}$ and $\sigma_{r'}\langle\Delta r'\rangle_{\mathrm{rot}}^{303\ \mathrm{K}}$ contribute around 2% or less to the total correction.

Turning to the contributions of the various terms in the *temperature evolution* of shieldings between 170 and 420 K, we note that the second order bending terms are even more important than in the case of a fixed temperature. Indeed, this contribution amounts to about half of the total temperature evolution for the terminal atoms and one-third for the central C atom. On the contrary, the other second order terms give small contributions. The excitation energies of the bending modes are (as usual) lower than those for the stretching modes, as seen from the harmonic frequencies in Table 1. The first order vibrational terms display an asymmetry so that the term involving the C=S bond (r') is always far more important the other one, reflecting an approximately three times larger *relative increase* of $\langle\Delta r'\rangle^T$ than $\langle\Delta r\rangle^T$ over the temperature range in question. And finally, the centrifugal terms are not negligible; they contribute up to 12% to the total temperature evolution.

D. ^{13}C Shielding—Temperature Dependence and Experimental Results

Following the approach described in Section III, we have performed all the density and temperature measurements (278–373 K) for gaseous OCS and CH_4. It enabled us to determine the ^{13}C magnetic shielding for each molecule extrapolated to zero density. The values of $\sigma_0(T)$ as functions of temperature are shown in Fig. 4 (curves (a) and (b)). These results describe the temperature dependence of isolated molecules, but still contain the unknown lock and reference contri-

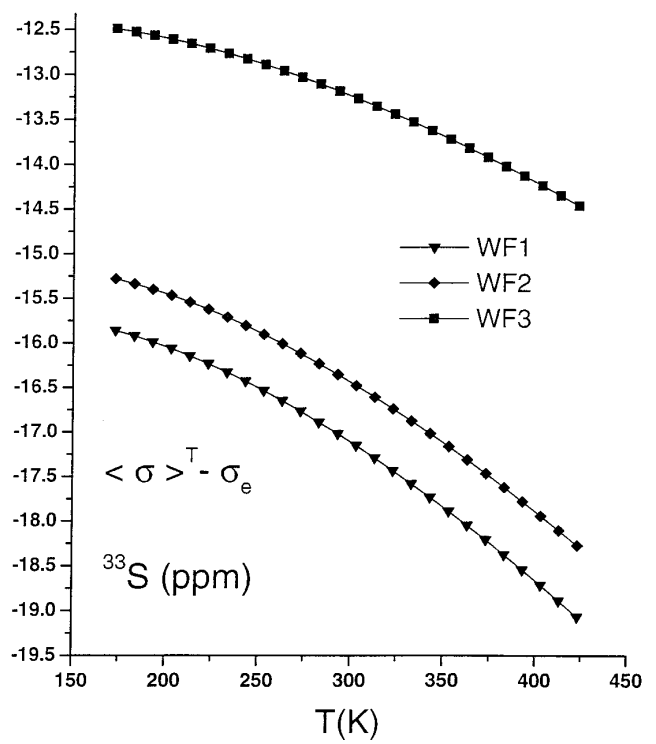

FIG. 3. Rovibrational contribution to the sulfur nuclear shielding constant in OCS as a function of temperature. Isotopomer $^{16}O{=}^{12}C{=}^{33}S$.

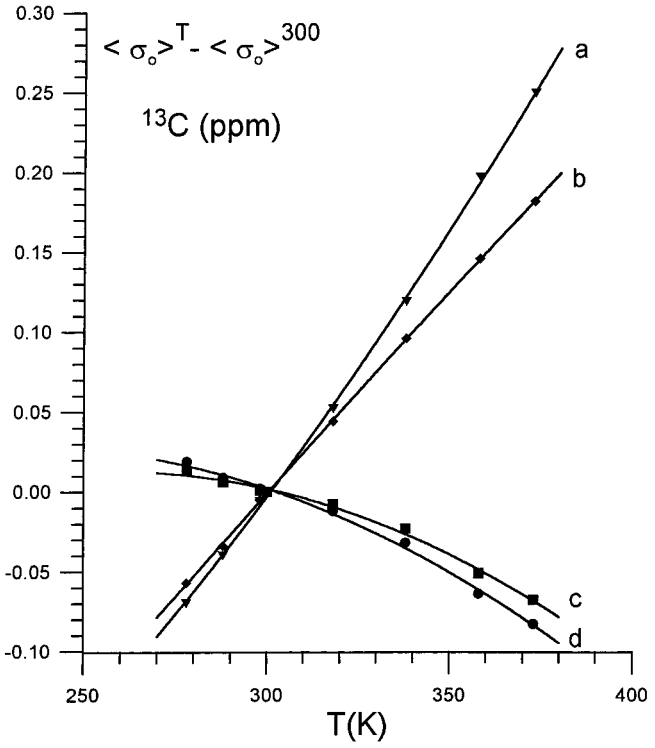

FIG. 4. Temperature dependence of ^{13}C magnetic shielding at the limit of zero density, $\sigma_0(T)$: (a) for CH_4 when toluene-d_8 is used for the lock and TMS frequency as the reference; (b) for OCS under the same experimental conditions; (c) for OCS measured relative to CH_4 ((b) − (a)); (d) for OCS as the absolute temperature dependence.

butions. These two factors were strictly the same for both CH_4 and OCS in our experiments. The ^{13}C shielding of OCS decreases with temperature when it is measured relative to CH_4, as shown by curve (c) in Fig. 4. The absolute temperature dependence of ^{13}C magnetic shielding in OCS is determined in the next step when the correction for the temperature dependence of shielding in CH_4 obtained by Raynes *et al.* (*1*) is included (curve (d) in Fig. 4). The final result can be expressed (in ppm) using the notation adopted by Jameson *et al.* (*45*) as

$$\langle\sigma_0\rangle^T - \langle\sigma_0\rangle^{300} = -7.74 \times 10^{-3}(T - 300) - 5.47 \times 10^{-6}(T - 300)^2 \qquad [5]$$

and it gives the absolute temperature dependence of ^{13}C magnetic shielding in an isolated OCS molecule. Figure 5 shows this function and the theoretically calculated temperature dependence. In the range of temperature investigated (278–373 K) the ^{13}C shielding of OCS is diminished by -0.104 ± 0.005 ppm, while the best ab initio calculation gives -0.105 ppm for the same range of temperature.

The excellent agreement of the experimental results with the ab initio values confirms the accuracy of the calculations for both molecules—OCS in this work and CH_4 in (*1*). It indicates also that even if we have not reached convergence of the calculated shielding constants with the basis set and correlation corrections, this does not affect the rovibrational effects. The remaining errors are apparently largely independent of the geometry; thus for each property surface further improvement of the calculation would affect mainly the point of reference (i.e., the equilibrium value).

We recall that the knowledge of the property surfaces enables also an estimate of all the isotope shifts. For example, at 300 K we find (WF3) for the change of carbon shielding on oxygen substitution $^1\Delta^{13}C$ ($^{17/16}O$) = −16 ppb, and similarly $^1\Delta^{13}C$ ($^{18/16}O$) = −31 ppb, where we have used the standard notation for the isotope shift.

E. Quadrupole Coupling

We have also computed the equilibrium and rovibrationally averaged ^{17}O and ^{33}S nuclear quadrupole coupling constants, $\chi(^{17}O)$ and $\chi(^{33}S)$. In this analysis of ^{17}O and ^{33}S quadrupole couplings, $^{17}O{=}{}^{12}C{=}{}^{32}S$ and $^{16}O{=}{}^{12}C{=}{}^{33}S$ isotopomers at 303 K were considered. For WF3, the results are $\chi(^{17}O)$, −1.089 and −1.084 MHz (rovibrationally averaged), and for $\chi(^{33}S)$, −31.76 and −31.46 MHz, respectively. The nuclear quadrupole moments used for ^{17}O and ^{33}S are -25.58×10^{-31} and -67.80×10^{-31} m^2, respectively (*46*). We can compare our results with other data: for ^{17}O, calculated −1.63 MHz (*14*) and experimental −1.32(14) MHz (*15*). For ^{33}S the calculated value is −29.91 MHz (*14*) and the experimental one is −29.118(1) MHz (*15*). We note, however, that our calculated electric field gradient for ^{33}S, −1.99344 a.u., is in very good agreement with the value of Ref. (*14*), −1.9888 a.u.; thus the above disagreement in $\chi(^{33}S)$ is due only to the use of a different nuclear quadrupole moment than in Ref. (*14*). For ^{17}O the corresponding electric field gradients are −0.18121 and −0.2690 a.u. We find that our values of $\chi(^{17}O)$ strongly depend on the basis set and MCSCF active space, whereas most of the values for $\chi(^{33}S)$ are close to the discussed WF3 result.

V. CONCLUSIONS

We have calculated in a fully ab initio approach the rovibrational effects on the shielding constants of all the nuclei in OCS. The accuracy of the calculated force field is confirmed by a comparison of our results with other theoretical and experimental data. Three different correlated wavefunctions were used for the shielding surfaces; thus we have an estimate of the role of the approximations in the theory. The shielding constants at the equilibrium geometry compare well with other results obtained applying correlated wavefunctions. The calculated rovibrational effects are applied to determine the temperature dependence of shielding constants, which may be directly compared with experiment. Apparently, the calculation of the relatively large difference between the shieldings at equilib-

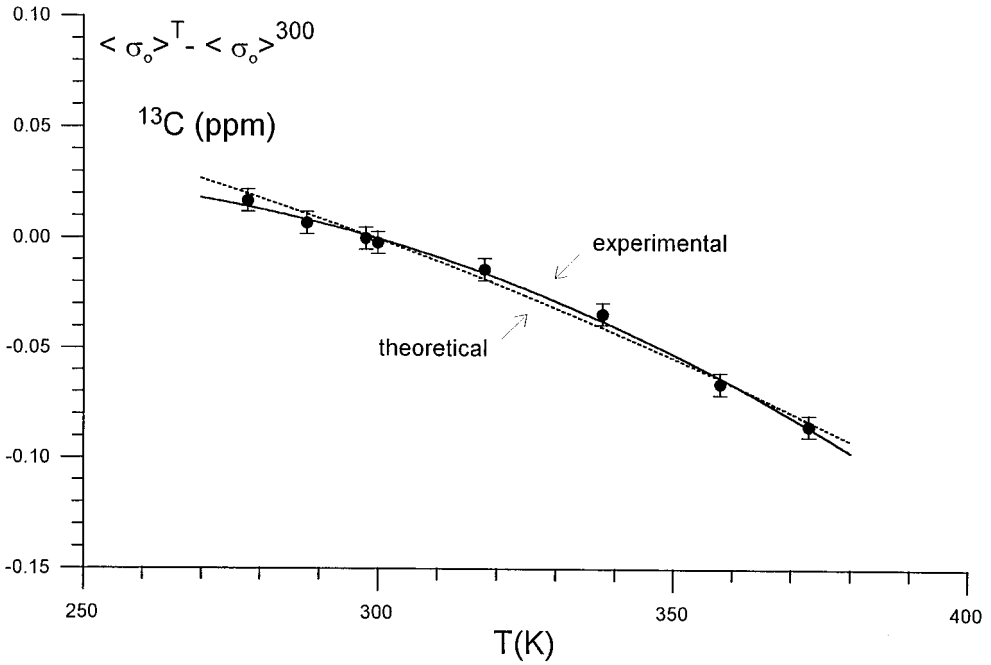

FIG. 5. A comparison of the experimental and calculated (WF3) temperature dependence of ^{13}C magnetic shielding in an isolated OCS molecule.

rium geometry and averaged for the lowest rovibrational level requires an accurate wavefunction. However, the much smaller relative changes in the experimentally accessible range of temperature are easier to compute and all our wavefunctions give practically the same results.

We present new and very accurate experimental data for the temperature dependence of ^{13}C shielding. The measured and calculated temperature dependence of ^{13}C shielding are in very good agreement. For the other nuclei, there is no reference standard, so in experiment we cannot establish the absolute temperature dependence in the same way. The accuracy of the ab initio results for carbon suggests that our calculated data for the temperature dependence of ^{17}O and ^{33}S shielding constants should be reliable, as also indicated by the similarity of the results obtained in all the three calculations performed. Therefore, these ab initio results could be applied as temperature reference functions for ^{17}O and ^{33}S NMR measurements. For ^{33}S shielding, we have in addition calculated the diamagnetic contribution. Combined with the known experimental spin–rotation constant, it provides an accurate value of absolute ^{33}S shielding in gas-phase OCS.

ACKNOWLEDGMENTS

This research was supported in part by the Polish Committee for Scientific Research as Project 12-501/03/BST-562/33/97 (K.J. and W.M.) and under Grant 3 T09A 133 09 (M.J.) and by the Nordisk Forskerutdanningsakademi (J.V.). The last author also thanks Professor Hans Ågren for his hospitality during the stay in Linköping University. K.J. acknowledges many helpful discussions with Professor Jukka Jokisaari and Dr. Petri Ingman during his visit to Oulu. We are indebted to Dr. Kenneth Ruud for the methane calculations and to Professor William T. Raynes for helpful discussions.

REFERENCES

1. W. T. Raynes, P. W. Fowler, P. Lazzeretti, R. Zanasi, and M. Grayson, *Mol. Phys.* **64,** 143 (1988).
2. A. K. Jameson, J. W. Moyer, and C. J. Jameson, *J. Chem. Phys.* **68,** 2873 (1978).
3. R. E. Wasylishen, S. Mooibroek, and J. B. Macdonald, *J. Chem. Phys.* **81,** 1057 (1984).
4. K. Jackowski, M. Jaszuński, and W. Makulski, *J. Magn. Reson.* **127,** 139 (1997).
5. T. H. Gierke and W. H. Flygare, *J. Am. Chem. Soc.* **94,** 7277 (1972).
6. A. K. Jameson and C. J. Jameson, *Chem. Phys. Lett.* **134,** 461 (1987).
7. A. J. Beeler, A. M. Orendt, D. M. Grant, P. W. Cutts, J. Michl, K. W. Zilm, J. W. Downing, J. C. Facelli, M. S. Schindler, and W. Kutzelnigg, *J. Am. Chem. Soc.* **106,** 7672 (1984).
8. R. E. Wasylishen, C. Connor, and J. O. Friedrich, *Can. J. Chem.* **62,** 981 (1984).
9. R. D. Amos and M. R. Battaglia, *Mol. Phys.* **36,** 1517 (1978).
10. M. Schindler, *J. Chem. Phys.* **88,** 7638 (1988).
11. J. Jokisaari, P. Lazzeretti, and P. Pyykkö, *Chem. Phys.* **123,** 339 (1988).
12. A. Bagno, *J. Mol. Struct. (THEOCHEM)* **418,** 243 (1997).
13. Ch. van Wüllen and W. Kutzelnigg, *J. Chem. Phys.* **104,** 2330 (1996).
14. K. A. Peterson, R. C. Mayhofer, and R. C. Woods, *J. Chem. Phys.* **94,** 431 (1991).
15. A. Maki and D. R. Johnson, *J. Mol. Spectrosc.* **47,** 226 (1973).
16. J. Lounila, J. Vaara, Y. Hiltunen, A. Pulkkinen, J. Jokisaari, M. Ala-Korpela, and K. Ruud, *J. Chem. Phys.* **107,** 1350 (1997).
17. F. London, *J. Phys. Radium* **8,** 397 (1937).

18. T. Helgaker and P. Jørgensen, *J. Chem. Phys.* **95,** 2595 (1991).
19. J. Gauss, *Chem. Phys. Lett.* **191,** 614 (1992).
20. J. Gauss, *J. Chem. Phys.* **99,** 3629 (1993).
21. D. B. Chesnut, *Chem. Phys. Lett.* **246,** 235 (1995).
22. J. Gauss and J. F. Stanton, *J. Chem. Phys.* **102,** 251 (1995).
23. J. Gauss and J. F. Stanton, *J. Chem. Phys.* **103,** 3561 (1995).
24. J. Gauss and J. F. Stanton, *J. Chem. Phys.* **104,** 2574 (1996).
25. D. Sundholm and J. Gauss, *Mol. Phys.* **92,** 1007 (1997).
26. J. Olsen and P. Jørgensen, *J. Chem. Phys.* **82,** 3235 (1985).
27. K. Ruud, T. Helgaker, R. Kobayashi, P. Jørgensen, K. L. Bak, and H. J. Aa. Jensen, *J. Chem. Phys.* **100,** 8178 (1994).
28. T. Helgaker, H. J. Aa. Jensen, P. Jørgensen, J. Olsen, K. Ruud, H. Ågren, T. Andersen, K. L. Bak, V. Bakken, O. Christiansen, P. Dahle, E. K. Dalskov, T. Enevoldsen, B. Fernandez, H. Heiberg, H. Hettema, D. Jonsson, S. Kirpekar, R. Kobayashi, H. Koch, K. V. Mikkelsen, P. Norman, M. J. Packer, T. Saue, P. R. Taylor, and O. Vahtras, Dalton, an ab Initio Electronic Structure Program, Release 1.0 (1997). See http://www.kjemi.uio.no/software/dalton/dalton.html.
29. S. Huzinaga, "Approximate Atomic Functions," Technical Report, University of Alberta, Edmonton (1971).
30. S. Huzinaga, *J. Chem. Phys.* **42,** 1293 (1965).
31. M. Schindler and W. Kutzelnigg, *J. Chem. Phys.* **76,** 1919 (1982).
32. A. Rizzo, T. Helgaker, K. Ruud, A. Barszczewicz, M. Jaszuński, and P. Jørgensen, *J. Chem. Phys.* **102,** 8953 (1995).
33. C. J. Jameson, *in* "Theoretical Models of Chemical Bonding. Part. 3. Molecular Spectroscopy, Electronic Structure, and Intramolecular Interactions" (Z. B. Maksic, Ed.), Springer-Verlag, Berlin/New York (1991).
34. A. R. Hoy, I. M. Mills, and G. Strey, *Mol. Phys.* **24,** 1265 (1972).
35. M. Toyama, T. Oka, and Y. Morino, *J. Mol. Spectrosc.* **13,** 193 (1964).
36. J. Lounila, R. Wasser, and P. Diehl, *Mol. Phys.* **62,** 19 (1987).
37. C. J. Jameson and H.-J. Osten, *J. Chem. Phys.* **81,** 2556 (1984).
38. A. D. Buckingham and J. A. Pople, *Disc. Faraday Soc.* **22,** 17 (1956).
39. C. J. Jameson, A. K. Jameson, and S. M. Cohen, *J. Chem. Phys.* **65,** 3397 (1976).
40. A. Rahman and M. I. Choudhary, "Solving Problems with NMR Spectroscopy," p. 109, Academic Press, San Diego (1996).
41. J. M. L. Martin, J.-P. Francois, and R. Gijbels, *J. Mol. Spectrosc.* **169,** 445 (1995).
42. Y. Pak and R. C. Woods, *J. Chem. Phys.* **107,** 5094 (1997).
43. Ch. van Wüllen, Ph.D. thesis, Ruhr-Universität Bochum (1992).
44. D. Sundholm, J. Gauss, and A. Schäfer, *J. Chem. Phys.* **105,** 11051 (1996).
45. C. J. Jameson, A. K. Jameson, and S. M. Cohen, *Mol. Phys.* **29,** 1919 (1975).
46. P. Pyykkö and J. Li, Report HUKI 1-92, Department of Chemistry, University of Helsinki (1992).
47. A. Foord, J. G. Smith, and D. H. Whiffen, *Mol. Phys.* **29,** 1685 (1975).
48. A. Fayt, R. Vandenhaute, and J. G. Lahaye, *J. Mol. Spectrosc.* **119,** 233 (1986).